Published in final edited form as:
Biochemistry. 2006 May 2; 45(17): 5468–5477.

Analysis of HIV-1 CRF_01 A/E Protease Inhibitor Resistance: Structural determinants for maintaining sensitivity and developing resistance to atazanavir

José C. Clemente[§], **Roxana M. Coman**, **Michele M. Thiaville**, **Linda K. Janka**, **Jennifer A. Jeung**, **Sarawut Nukoolkarn**[‡], **Lakshmanan Govindasamy**, **Mavis Agbandje-McKenna**, **Robert McKenna**, **Wichet Leelamanit**[‡], **Maureen M. Goodenow**[†], and **Ben M. Dunn**[*]

[§] *Johnson & Johnson Pharmaceutical Research & Development, LLC, 665 Stockton Dr. Exton, PA 19341, University of Florida College of Medicine Department of Biochemistry and Molecular Biology, Gainesville, Florida 32610* [†] *Department of Pathology, Immunology, and Laboratory Medicine, Gainesville, Florida 32610* [‡] *Department of Biochemistry, Faculty of Pharmacy, Mahidol University, 447 Sri-Ayuthaya Rd., Bangkok 10400, Thailand*

Abstract

A series of HIV-1 protease mutants have been designed to analyze the contribution to drug resistance provided by natural polymorphisms as well as therapy-selective (active and non-active site) mutations in the HIV-1 CRF_01 A/E (AE) protease when compared to the subtype-B (B) protease. Kinetic analysis of these variants using chromogenic substrates showed differences in substrate specificity between pre-therapy B and AE proteases. Inhibition analysis with ritonavir, indinavir, nelfinavir, amprenavir, saquinavir, lopinavir, and atazanavir revealed that the natural polymorphisms found in A/E can influence inhibitor resistance. It was also apparent that a high level of resistance in the A/E protease, as with B protease, is due to aquiring a combination of active site and non-active site mutations. Structural analysis of atazanavir bound to a pre-therapy B protease showed that the ability of atazanavir to maintain its binding affinity to variants containing some resistance mutations is due to its unique interactions with flap residues. This structure also explains why the I50L and I84V mutations are important in decreasing the binding affinity of atazanavir.

Introduction

The genetic variability encountered in the Human Immunodeficiency Virus (HIV) poses a major challenge for the world health care community. There are two main types of HIV, Type-1 (HIV-1) and Type-2 (HIV-2), with HIV-1 being the most prevalent in the world wide pandemic. HIV-1 has been classified into three groups, M, N, and O. Viruses in group M are further subdivided into subtypes, sub-subtypes, and recombinant forms (CRFs), which are prevalent in specific geographical regions. The subtype-B virus is common to the Americas, Europe, and Australia. Non-subtype-B viruses dominate the growing epidemic in the developing world (World Health Organization).

The nucleotide diversity between protease subtypes and CRFs map to all regions of the viral genome including the genes encoding the therapeutic targets protease and reverse transcriptase. Many of these polymorphisms are manifested as amino acid mutations in the protease at

*To whom correspondence should be addressed. Phone: (352) 392-3362, Fax: (352) 846-0412, email: bdunn@ufl.edu.

positions that are common variants in Subtype-B viruses in response to protease inhibitor (PI) therapy. The currently available therapeutic protease inhibitors were developed and tested only against the Subtype-B (B) protease. There are limited data confirming that different HIV-1 subtypes and CRFs are more or less susceptible to the various protease inhibitors (1). It would be expected that the worldwide use of protease inhibitors would impart further selective pressure driving the evolution of HIV-1. The residue polymorphisms in the protease have raised concerns that the therapy of non-B viruses may be less effective than for subtype B viruses (2–5).

In this study we aimed to analyze the effects on biochemical properties, specifically substrate specificity and inhibitor binding, by natural polymorphisms in the CRF_01 A/E (AE) protease and therapy-selected active and non-active site mutations when compared to B protease. We determined the Michaelis-Menten constants for three substrates and K_i value for seven available therapeutic PIs against a pre-therapy B protease a pre-therapy isolated AE protease containing the natural polymorphisms V3I, I13V, E35D, M36I, S37N, R41K, H69K, and L89M, and the post-therapy AE (AE-P) protease isolated from a patient treated with saquinavir (SQV), ritonavir (RTV), and indinavir (IDV) PI therapy, Figure 1 (6).

To determine the effects of the active site mutation V82F and the natural polymorphisms in AE protease on substrate specificity and inhibitor susceptibility, the V82F mutation was added to B (B^{V82F}) and AE (AE^{V82F}) proteases. To assess the effects of the therapy-selected non-active site mutations, the V82F mutation in AE-P was back mutated to pre-therapy ($AE\text{-}P^{F82V}$) protease. During the course of our study it was evident that atazanavir (ATV) was able to maintain its binding affinity to all mutants. In order to understand the mechanism utilized by ATV to maintain its binding affinity to resistant proteases, we have determined the X-ray crystal structure of ATV bound to the pre-therapy B protease.

Experimental Procedures

Mutagenesis and Expression of Protease

A complete description of the cloning, expression, and purification procedures can be found in Ido et al. and Goodenow et al. (7,8). In brief, the HIV-1 protease DNA for all the HIV B and AE variants were sub-cloned into the pET23a expression vector (Novagen) (9). The construct was transformed into the *E. coli* strain BL21 Star DE3 PlysS from Invitrogen. The introduction of all mutations onto the B and AE background were done using the QuikChange™ Mutagenesis Kit from Stratagene. Protease expression in bacteria was initiated when the OD_{600} reached 0.6 by addition of 1mM IPTG to a culture grown at 37°C in M9 Media (6.8 g Na_2HPO_4, 3 g KH_2PO_4, 0.5 g NaCl, 1 g NH_4SO_4, and 5 g Casamino Acids were autoclaved together in 987 ml of H_2O, then 1 ml of 0.1 M $CaCl_2$, 2 ml of 1.0 M $MgSO_4$, 10 ml of 20% glucose, and 50 μg/L of Ampicillin were added). After three hours, cells were harvested by centrifugation at 16,000 × g for five minutes and resuspended in TN buffer (0.05 M Tris. 0.15 M NaCl, 0.001 M $MgCl_2$, pH 7.4). Inclusion bodies containing the protease were isolated by centrifugation through a 27% sucrose cushion. The inclusion bodies were solubilized in 8M urea and the protease was refolded by dialysis against 0.05 M sodium phosphate buffer (0.05 M Na_2HPO_4, 0.005 M EDTA, 0.3 M NaCl, and 0.001 M dTT, pH 7.3). The protease was purified through ammonium sulfate precipitation and gel filtration chromatography using a Superdex 75 16/60 column from Amersham Pharmacia attached to an FPLC LCC 500 Plus, also from Pharmacia. The protease was eluted using potassium phosphate buffer (50 mM K_2HPO_4, 2 mM EDTA, 150 mM NaCl, 2 mM dTT, 5% glycerol, and 5% isopropanol, pH 7.3).

Protease Activity and Inhibitor Constants

The Michaelis-Menten constants k_{cat}, K_m, and k_{cat}/K_m and K_i values were determined for each variant as previously described (10). The chromogenic substrates K-A-R-V-*L**Nph-E-A-nL-G (S1), K-A-R-V-*nL**Nph-E-A-nL-G (S2), and K-A-R-V-*F**Nph-E-A-nL-G (S3) which mimics the CA/p2 cleavage site, were used to determine the catalytic activity of each variant at 37°C in sodium acetate buffer (0.05 M NaOAc 0.15 M NaCl, 0.002 M EDTA, 0.001 M DTT, pH 4.7). The P1 residue was substituted with the residues leucine (Leu), nor-leucine (nLeu), and phenylalanine (Phe). These three residues were analyzed because they are commonly found in the P1 position of the Gag-Pol cleavage sites. Nor-leucine is used to mimic the volume occupied and hydrophobicity of methionine (Met) while avoiding any problems due to oxidation of the sulfur. K_i values for all inhibitors were measured under the same conditions. Cleavage of the substrate was monitored using a Hewlett Packard 8452A spectrophotometer equipped with a 7-cell sample handling system as described by Dunn et al. (11). The inhibition constants K_i were determined by monitoring the inhibition of hydrolysis of the chromogenic substrate as described by Bhatt et al. (12).

Relative Vitality

To better describe the effect resistance mutations have on virus viability in the presence of a specific inhibitor Gulnik *et al.* introduced the vitality parameter that is described by the following equation (13):

$$Vitality = \frac{(K_i * k_{cat}/K_m)_{mutant}}{(K_i * k_{cat}/K_m)_{wild-type}}$$

Because some second generation inhibitors have low picomolar binding constants, a ten-fold drop in affinity will still leave an inhibitor with a sub-nanomolar binding constant. This inhibitor would still be able to arrest viral maturation since it would be able to out-compete the substrate. To better describe the effects of these inhibitors, Velazquez-Campoy (1) introduced a modified vitality value, which is normalized to a reference inhibitor, termed relative vitality described by the following equation:

$$RelativeVitality = \frac{(K_i * k_{cat}/K_m)_{mutant}}{(K_i)_{referenceInhibitor} * k_{cat}/K_m)_{wild-type}}$$

Crystallization of Protein-Inhibitor Complex

After protease B was purified, the enzyme purification buffer was exchanged for 50 mM sodium acetate, 1mM EDTA, and 1 mM DTT at pH 4.7 during concentration to 2 mg/ml. Atazanavir was dissolved at a concentration of 20 mM in 100% DMSO and mixed with B protease in a molar ratio of 3:1. The inhibitor and enzyme were allowed to equilibrate for one hour at 4° C after which precipitated material was removed by centrifugation at 10,000× g at 4° C. The enzyme-inhibitor complex was mixed with reservoir solution (Hampton Research Cryo Crystallization Kit #18) in a 1:1 (v/v) ratio to set up 4 μL hanging drops at 25° C. Rod shaped crystals grew in two days.

Data Collection, Structure Determination, and Refinement

X-ray diffraction images were collected at the Brookhaven National Laboratory beamline X29 on an ADSC quantum 315 CCD detector. The crystal was dipped in cryoprotectant solution (30% glycerol in reservoir solution) prior to data collection at 100° K. A complete data set, from 65 images taken with 1.0° oscillation steps with 5 s exposures, was collected from a single crystal. The data were indexed, scaled, and reduced using DENZO and SCALEPACK, (14). The complex crystallized in the $P6_1$ space group with unit cell dimensions a = 62.4 and c = 82.6 Å.

Initial phases were calculated using the coordinates of B protease, PDB entry 1SGU, after removal of inhibitor and solvent molecule to avoid model phase bias. Standard methods of structure refinement were then employed using programs in the CNS Suite (15). Electron density maps with coefficients $2F_o-F_c$ and F_o-F_c were used to guide manual fitting of the protease and bound inhibitor followed by real space refinement using the molecular graphics program WinCoot, (16). The inhibitor and water molecules were added into F_o-F_c density at 3σ. During model building and refinement, 5% of the data was reserved for cross validation of the refinement progress. The atomic coordinates have been deposited in the Protein Data Bank: 2AQU.

Results and Discussion

The aim of this study was to analyze the contributions to catalytic efficiency and inhibitor resistance by natural background polymorphisms and therapy-selected, active and non-active site, residue changes in AE compared to B protease, Figure 1. Though the natural polymorphisms found in AE when compared to the B protease have arisen in the absence of PI therapy, residue changes in AE at positions 35, 36, 37, 41, 69, and 89 have been associated with PI resistance in vivo and in vitro in B proteases (17–20). Thus, these polymorphisms can potentially influence substrate processing and the binding of currently available PIs and/or facilitate the development of resistance.

Michaelis-Menten Constants

The Michaelis-Menten constants were determined for three substrates with each variant in order to assess the effects of natural polymorphisms and drug selected mutations on substrate specificity and are shown in Table 1. Of the substrates tested, the B and AE proteases preferred phenylalanine at the P1 position (S3 substrate). Phenylalanine is the most common residue found at the P1 position occurring in 40% of cleavage sites in GagPol. Methionine and leucine occur in 10 and 20% of cleavage sites, respectively. Though there is a preference by both proteases for phenylalanine, the differences seen in the Michaelis-Menten constants for all substrates suggest that the natural polymorphisms in AE can influence active site specificity and/or catalytic efficiency. In contrast to the data reported earlier for subtype-C (C) and –A (A) proteases, the AE protease does not show any clear catalytic advantage over B protease (21).

Additional evidence for the effects of the natural polymorphisms and active and non-active site therapy-selected mutations affecting substrate specificity can be seen when comparing the kinetic values for the variants B^{V82F}, AE^{V82F}, AE-P, and AE-P^{F82V}, Table 1. These variants showed a decrease in k_{cat}/K_m for all substrates when compared to the pre-therapy proteases. A clear example of the effects on substrate binding and catalytic efficiency by the natural polymorphisms in AE can be seen when comparing the Michaelis-Menten parameters for the S3 substrate and the AE^{V82F} and B^{V82F} variants. Both proteases showed similar k_{cat}/K_m values for S3 (AE^{V82F}, $k_{cat}/K_m = 0.33$; B^{V82F}, $k_{cat}/K_m = 0.38$). While the AE^{V82F} was able to maintain a similar k_{cat} (14 sec^{-1}) value as that for AE (15 sec^{-1}), the B^{V82F} protease showed a decrease in k_{cat} of 30% (9.0 sec^{-1} to 6.4 sec^{-1}) when compared to B. Similar differences between the contributing parameters to k_{cat}/K_m were seen for all the substrates with B^{V82F} and AE^{V82F}.

It is also apparent that the natural polymorphisms in AE alone do not provide an advantage for substrate catalysis in combination with the primary active site mutation V82F. Comparing the AE, AE^{V82F}, AE-P, and AE-P^{F82V} proteases revealed that adding the therapy-selected non-active site mutations (AE-P, $k_{cat}/K_m = 1.0\ \mu M^{-1}sec^{-1}$) improved catalytic efficiency when compared to AE^{V82F} ($k_{cat}/K_m = 0.33\ \mu M^{-1}sec^{-1}$), but removal of the active site mutation (AE-P^{F82V}, $k_{cat}/K_m = 0.5\ \mu M^{-1}sec^{-1}$) did not restore wild type activity (AE, $k_{cat}/K_m = 1.7\ \mu M^{-1}sec^{-1}$). These data clearly displayed cooperativity between the active site and post-

therapy non-active site mutations to improve or maintain catalytic efficiency. As shown by other studies on B proteases, these cooperative effects between active site and non-active site mutations to improve catalytic efficiency are clearly not independent (10,22,23).

Inhibitor Dissociation Constants

The K_i values for all variants against seven clinically used inhibitors are shown in Table 2, and all fold changes are a comparison to the B protease. Fold changes to other proteases are specifically stated.

Velazquez-Campoy et al. (2003) showed that C and A proteases were 2- to 7-fold less susceptible to inhibition by clinically used inhibitors when compared to B protease (24). The AE protease showed no greater than 2-fold increase in K_i to any of the inhibitors tested, Table 2. The effects on inhibitor binding by the V82F mutation on the wild type background of B and AE varies from none to significant (>10 fold) and varies between subtypes. The B^{V82F} showed a 15-fold increase in K_i for APV while the AE^{V82F} mutant showed a 12- and 35-fold increase in Ki for lopinavir (LPV) and IDV, respectively. The decrease in sensitivity of AE^{V82F} to IDV and LPV and B^{V82F} to amprenavir (APV) inhibition compared to B predicts a predisposition to developing resistance to these three inhibitors by the AE or B proteases. Although LPV, IDV, and APV exhibited a decrease in activity against AE^{V82F} or B^{V82F}, it is not a clear marker of resistance, since LPV and APV maintained a binding strength sufficient for effective inhibition of the protease when using IDV against the pre-therapy proteases as a gauge. To better determine the viability of viruses containing these mutations, we analyzed the variants using relative vitality as described in the Materials and Methods section. The results for the S1 substrate are shown in Figure 2A and B. The results for S2 and S3 mimic that of S1, therefore they have been excluded. When using relative vitality values as a comparison only IDV is predicted to have a decreased potency against a virus carrying the AE^{V82F} variant when compared to AE and B, Figure 2A. These data predict that the natural polymorphisms found in the AE protease can select for faster development of IDV resistance upon the acquisition of the V82F mutation.

The post-therapy AE-P protease showed up to a ~500-fold increase in K_i for the inhibitors tested. Analysis of relative vitality values for these inhibitors with AE-P also predicts a large degree of cross-resistance, Figure 2B. Atazanavir showed no decrease in potency though the AE-P protease contains mutations at five residues (10, 33, 36, 54, and 82) associated with resistance to this inhibitor (25). It is of interest that ATV has remained highly potent against an enzyme that showed ~20- to 500-fold decrease in binding affinity to the other six inhibitors tested, and this will be discussed further below.

Back mutating the active site mutation V82F in AE-P ($AE\text{-}P^{F82V}$) removed a significant level of the cross resistance to the inhibitors RTV, IDV, nelfinavir (NFV), APV, and LPV when compared to AE-P, Table 2. The $AE\text{-}P^{F82V}$ and AE^{V82F} proteases show similar susceptibility to RTV, APV, and LPV. The $AE\text{-}P^{F82V}$ variant showed a 5- and 100-fold greater susceptibility to NFV and SQV, respectively, when compared to AE^{V82F}. The AE^{V82F} showed a 3-fold greater susceptibility to IDV compared to $AE\text{-}P^{F82V}$. As with substrate binding and processing, it is evident that both active and non-active site mutations have the ability to alter the binding of inhibitors to the active site. It is apparent that independently active or non-active site mutations (AE^{V82F} and $AE\text{-}P^{F82V}$) do not provide for a high level of cross-resistance when compared to the AE-P protease. As seen with B proteases, comparison of the three variants, AE-P, $AE\text{-}P^{F82V}$, and AE^{V82F} show cooperativity between therapy-selected active and non-active site mutations leading to a high level of resistance and cross-resistance (10,22,23,26, 27). It is also apparent that the cooperative contributions to resistance by active and non-active site mutations are not independent and are not additive but multiplicative.

Structural analysis of ATV binding

To analyze the possible interactions that permits ATV to be the only PI that is able to maintain its binding affinity to all proteases studied, Table 2., the crystal structure of ATV bound to the B protease (B-ATV) was determined. Attempts to crystallize the AE variants were unsuccessful. The B-ATV complex X-ray crystallographic data and refinement statistics are given in Table 3. Density for two binding modes of the inhibitor was observed in the active site of the protease, Figure 3A. This is indicative of a 2-fold (180°) bi-module binding of the inhibitor and has previously been observed for other inhibitors (28). Weak density was observed for the pyridine ring occupying the S3 or S3′ pockets in the two conformations (Conf1 and Conf2) of the inhibitor indicative of disorder in this region consistent with the high B-factors for the pyridine atoms, Figure 3B. Both inhibitor conformations displayed an average B-factor of 28 $Å^2$.

Hydrophobic interactions between ATV and the protease were analyzed using the program Ligplot, Figure 4 (29). Due to the fact that the HIV-1 protease is a homodimer the naming of chain (A) and (B) is arbitrary for each monomer in the case where two inhibitor conformations are seen. In this study we have assigned the enzyme subsites S3, S1, and S2′ to be formed by the residues in chain A, Figure 4B, and subsites S2, S1′, and S3′ to be formed by residues in chain B. Given this structural assignment the inhibitor group 4-(pyridin-2-yl)phenyl occupies the S1 and S3 pockets in Conf1 and the S1′ and S3′ pockets in Conf2. Residue Ile47 was found in two conformations. Only the conformation of Ile47 with atoms within 4 Å of the inhibitor was analyzed.

None of the proteases analyzed contain the I50L or I84V mutations, which are associated with a high level of ATV resistance in vivo and in vitro (30–32). The Ile50 residue forms various interactions to lock down the flaps and mutations at this residue may function to destabilize the protease closed conformation (23). The Ile84 residue is located in the center of the active site and we previously suggested that the I84V mutation may function to destabilize the interactions of the core of the inhibitor and its interactions with the flaps (23). Previous studies have also shown the importance of mutations in the flaps in providing a high level of resistance (10,22,23,26), and that the addition of non-active site mutations may decrease binding affinity by destabilizing the flaps in the bound conformation decreasing binding affinity (23). Recent studies by Yanchunas and colleagues, utilizing thermodynamic and modeling techniques, have suggested the importance of ATV P2 and P2′ groups interactions with Ile50 in maintaining binding affinity (33). We can see from the analysis of B-factor values of the bound ATV that the most stable regions are the P2 and P2′ N-methoxycarbonyl-L-*tert*-leucine groups, Figure 4B. The P2 and P2′ groups make hydrophobic contacts with Ile47and Ileu50 (flaps) and Ile84 (active site). Knowing the correlation between drug resistance and flap function, the strong interactions that ATV P2 and P2′ groups make with the flap residues may provide for its ability to bind to resistant proteases containing numerous mutations. Given the key resistance mutations found in response to ATV, it appears that resistance to ATV is associated with weakening the interactions of the N-methoxycarbonyl-L-*tert*-leucine group and destabilizing the flap interactions.

Atazanavir makes a total of 11 (Conf1) and 12 (Conf2) hydrogen bonds with the enzyme. Two of these H-bonds are with the flap residue Gly48, Figure 5A and 5B. The G48V mutation is found in proteases isolated from therapy experienced patients after treatment with ATV. The residue 48Val side chain points away from the inhibitor and does not make contact with ATV (34, 35). No other residue with which ATV makes a direct H-bond is associated with resistance to any clinical inhibitor. Hong et al showed that mutations at position 48 provide inhibitor resistance by decreasing the flexibility of the flaps. In the case of ATV, the G48V mutation may function to destabilize the H-bonds, and cooperatively increase resistance with additional

mutations. This further supports the prediction that the destabilization of the interactions of the flaps and ATV is important for developing resistance.

When compared to previously reported wild type-inhibitor complex structures of the HIV-1 protease, ATV is unique in that it binds in two conformations with each conformation making unique H-bonding and hydrophobic interactions (28,36–39). Analysis of the structure showed a substantial amount of hydrophobic and H-bonding interactions, thus it is apparent why ATV binds with a highly favorable enthalpy (33,40). A large part of the binding affinity of ATV to wild type protease comes from the large number of H-bonds it makes with the enzyme. The two inhibitor conformations make equivalent direct H-bonds involving backbone atoms, but differ in their water (Wat) mediated H-bonds, Figure 5A and 5B. The Conf1 and Conf2 inhibitor form three and four waters mediated H-bonds, respectively, bridging the enzyme and the inhibitor. The H-bond between the N6 atom of the 4-(pyridin-2-yl)phenyl group with Wat73 in Conf1 is mediated by Wat9 in Conf2. The Wat9 water molecule is also within hydrogen bonding distance to NH1 of Arg8(B). Additional differences in H-bonding between the two inhibitor conformations can be seen in the ability of Wat9 to H-bond to Wat66, forming a H-bonding water chain involving two additional waters and ending at the NE atom of Arg87(A).

The disorder in Ile47(B) coincides with the Wat71 mediated H-bonding between O1 and O2 of the methoxycarbonyl group in Conf1 and Conf2, respectively, with Gly48(B), Figure 5A and 5B. Given the symmetry of ATV it is surprising that this H-bonding interaction is not observed with residue Gly48(A) at the other end of the inhibitor. It is difficult to determine if the H-bonding interaction mediated by Wat71 with Gly48(B) is in both inhibitor conformations or in only one. If it is found in both, then the interactions are distinctly different. In Conf1 the H-bond involves the methoxycarbonyl-L-*tert*-leucine opposite the 4-(pyridin-2-yl)phenyl group, while in Conf2 it is opposite to the phenyl group. Given that juxtaposed groups will influence each other's interaction with the enzyme, the disorder of Ile47(B) may be due to differences in its interactions with each inhibitor conformation. It is possible that this water mediated H-bonding interaction is only possible in one inhibitor conformation (41). If this is so then the interactions of Conf1 and Conf2 with the enzyme can also be said to be different.

As with hydrogen bonding interactions, the hydrophobic interactions are unique between the two inhibitors. Atazanavir in Conf1 and Conf2 make a total of 27 (14 chain A and 13 chain B) and 28 (14 with chain A and 14 chain B) hydrophobic contacts, respectively, Figure 4A. The two inhibitor conformations interact with similar residues but in the opposite chain. The main difference is in the interactions of the 4-(pyridin-2-yl)phenyl group. The 4-(pyridin-2-yl)phenyl group of Conf1 make hydrophobic contacts with residues Pro81(A), Val82(A), Ile84(A), Gly48 (B), and Gly49(B) for a total of nine hydrophobic contacts. The 4-(pyridin-2-yl)phenyl group of Conf2 make hydrophobic contacts with residues Gly48(A), Gly49(A) and Pro81(B), for a total of five hydrophobic contacts. Unlike Conf1, this side chain group in Conf2 does not make contact with residues Val82(B) and Val84(B).

Analysis of residue Val32 interactions revealed additional flexibility in the binding of ATV. Residues Val32(A) (S2 pocket) and Val32(B) (S2′ pocket) in the active site occupy different conformations due to a 180° rotation around the Cα-Cβ bond, Figure 6. The average distance of L-*tert*-leucine atoms to the γC2 of Val32(A) and γC1 of Val32(B) for Conf1 are 4.9 Å and 4.4 Å, respectively. The average distance of L-*tert*-leucine atoms to the γC2 of Val32(A) and γC1 of Val32(B) for Conf2 are 4.8 Å and 4.2 Å, respectively. The difference in the orientation of residue 32 coincides with the alternate conformations of residue Ile47(B) described above. The γC2 of Val32(A) makes van der Waals contacts with the δC of Ile47(A). In chain B this interaction is lost. In chain B the γC1 of Val32(B) makes van der Waals contacts with Ile84 (B). It would be expected that the structural differences in chains A and B surrounding Val32 affecting inhibitor-enzyme hydrophobic interactions are different for the two inhibitor

conformations. These differences are due to the distinct P1 and P1′ groups found opposite the S2 and S2′ pockets for each inhibitor conformation, and the alternate conformations of Ile47 (B). It is possible that the alternate conformations of Ile47(B) is due to the conformation of Val32(B). Valine32 in chain A and B also showed alternate levels of interactions with residue Ile84, which forms the juncture between the S1 and S2′, and S1′ and S2 pockets. Differences in the interactions of Val32 and Ile84 will also affect the interactions between Ile84 and the inhibitors.

Conclusions

The current pattern of resistance development by HIV to protease inhibitors is the acquisition of protease active site mutation followed by several non-active site accessory mutations. It was originally believed that non-active site mutations were acquired to regain the loss of catalytic activity due to active site mutations. Recent studies from our laboratory and others have shown that many non-active site mutations in HIV-1 subtype-B proteases will contribute to decreasing the binding affinity of inhibitors, while maintaining catalytic efficiency (10,22–24,26,27). In this study we provide insights into the effects of natural polymorphisms and the contributions to resistance made by therapy-selected active site and non-active site mutations found in the CRF_01 AE protease. We have also established the structural determinants for the unique ATV resistance associated mutation I50L, and the ability of ATV to maintain its binding affinity to cross-resistant proteases.

Acknowledgements

We would like to thank Dr. Rebecca E. Clemente for her help editing this manuscript. We would like to thank the following for gifts of the HIV protease inhibitors: Abbott Laboratories (ritonavir), Merck (indinavir), Agouron now Pfizer (nelfinavir), and the NIH AIDS Research and Reference Reagent Program (saquinavir, lopinavir, amprenavir, and atazanavir).

Funding: This work was supported by grants from the NIH (AI28571 to B.M.D and M. M. G. and Post-Doctoral Fellowship from Training Grant T32 CA09126 to J.C.C.)

Abbreviations used

HAART
: highly active antiretroviral therapy

IPTG
: isopropylthio-D-galactopyranoside

A_{600}
: absorbance at 600 nm

dTT
: dithiothreitol

Nph
: p-NO_2 -L-phenylalanine

nL
: L-norLeucine

PI
: protease inhibitor

RTV
: Ritonavir

IDV
Indinavir

NFV
Nelfinavir

SQV
Saquinavir

APV
Amprenavir

LPV
Lopinavir

ATV
Atazanavir

H-bonds
hydrogen bonds

B
pre-therapy HIV-1 subtype-B protease

AE
pre-therapy HIV-1 CRF_01 A/E protease

B^{V82F}
B protease plus active site mutation V82F

AE^{V82F}
AE protease plus active site mutation V82F

AE-P
post-therapy HIV-1 CRF_01 A/E protease

AE-P^{F82V}
AE-P protease with back mutation F82V

References

1. Velazquez-Campoy A, Vega S, Freire E. Amplification of the effects of drug resistance mutations by background polymorphisms in HIV-1 protease from African subtypes. Biochemistry 2002;41:8613–9. [PubMed: 12093278]
2. Pieniazek D, Rayfield M, Hu DJ, Nkengasong J, Wiktor SZ, Downing R, Biryahwaho B, Mastro T, Tanuri A, Soriano V, Lal R, Dondero T. Protease sequences from HIV-1 group M subtypes A-H reveal distinct amino acid mutation patterns associated with protease resistance in protease inhibitor-naive individuals worldwide. HIV Variant Working Group. Aids 2000;14:1489–95. [PubMed: 10983635]
3. Vergne L, Peeters M, Mpoudi-Ngole E, Bourgeois A, Liegeois F, Toure-Kane C, Mboup S, Mulanga-Kabeya C, Saman E, Jourdan J, Reynes J, Delaporte E. Genetic diversity of protease and reverse transcriptase sequences in non-subtype-B human immunodeficiency virus type 1 strains: evidence of many minor drug resistance mutations in treatment-naive patients. J Clin Microbiol 2000;38:3919–25. [PubMed: 11060045]
4. Cornelissen M, van den Burg R, Zorgdrager F, Lukashov V, Goudsmit J. pol gene diversity of five human immunodeficiency virus type 1 subtypes: evidence for naturally occurring mutations that contribute to drug resistance, limited recombination patterns, and common ancestry for subtypes B and D. J Virol 1997;71:6348–58. [PubMed: 9261352]

5. Grossman Z, Vardinon N, Chemtob D, Alkan ML, Bentwich Z, Burke M, Gottesman G, Istomin V, Levi I, Maayan S, Shahar E, Schapiro JM. Genotypic variation of HIV-1 reverse transcriptase and protease: comparative analysis of clade C and clade B. Aids 2001;15:1453–60. [PubMed: 11504976]
6. Nukoolkarn S, Pongthapisith V, Panyim S, Leelamanit W. Sequence variability of the HIV type 1 protease gene in thai patients experienced with antiretroviral therapy. AIDS Res Hum Retroviruses 2004;20:1368–72. [PubMed: 15650431]
7. Ido E, Han HP, Kezdy FJ, Tang J. Kinetic studies of human immunodeficiency virus type 1 protease and its active-site hydrogen bond mutant A28S. J Biol Chem 1991;266:24359–66. [PubMed: 1761538]
8. Goodenow MM, Bloom G, Rose SL, Pomeroy SM, O'Brien PO, Perez EE, Sleasman JW, Dunn BM. Naturally occurring amino acid polymorphisms in human immunodeficiency virus type 1 (HIV-1) Gag p7(NC) and the C-cleavage site impact Gag-Pol processing by HIV-1 protease. Virology 2002;292:137–49. [PubMed: 11878916]
9. Wain-Hobson S, Sonigo P, Danos O, Cole S, Alizon M. Nucleotide sequence of the AIDS virus, LAV. Cell 1985;40:9–17. [PubMed: 2981635]
10. Clemente JC, Hemrajani R, Blum LE, Goodenow MM, Dunn BM. Secondary mutations M36I and A71V in the human immunodeficiency virus type 1 protease can provide an advantage for the emergence of the primary mutation D30N. Biochemistry 2003;42:15029–35. [PubMed: 14690411]
11. Dunn BM, Gustchina A, Wlodawer A, Kay J. Subsite preferences of retroviral proteinases. Methods Enzymol 1994;241:254–78. [PubMed: 7854181]
12. Bhatt D, Dunn BM. Chimeric aspartic proteinases and active site binding. Bioorg Chem 2000;28:374–93. [PubMed: 11352473]
13. Gulnik SV, Suvorov LI, Liu B, Yu B, Anderson B, Mitsuya H, Erickson JW. Kinetic characterization and cross-resistance patterns of HIV-1 protease mutants selected under drug pressure. Biochemistry 1995;34:9282–7. [PubMed: 7626598]
14. Otwinowski, Z.; Minor, W. Macromolecular Crystallography. 1997. p. 307-326.
15. Brunger AT, Adams PD, Clore GM, DeLano WL, Gros P, Grosse-Kunstleve RW, Jiang JS, Kuszewski J, Nilges M, Pannu NS, Read RJ, Rice LM, Simonson T, Warren GL. Crystallography & NMR system: A new software suite for macromolecular structure determination. Acta Crystallogr D Biol Crystallogr 1998;54(Pt 5):905–21. [PubMed: 9757107]
16. Emsley P, Cowtan K. Coot: model-building tools for molecular graphics. Acta Crystallogr D Biol Crystallogr 2004;60:2126–32. [PubMed: 15572765]
17. Rusconi S, La Seta Catamancio S, Citterio P, Kurtagic S, Violin M, Balotta C, Moroni M, Galli M, d'Arminio-Monforte A. Susceptibility to PNU-140690 (Tipranavir) of human immunodeficiency virus type 1 isolates derived from patients with multidrug resistance to other protease inhibitors. Antimicrob Agents Chemother 2000;44:1328–32. [PubMed: 10770770]
18. Patick AK, Mo H, Markowitz M, Appelt K, Wu B, Musick L, Kalish V, Kaldor S, Reich S, Ho D, Webber S. Antiviral and resistance studies of AG1343, an orally bioavailable inhibitor of human immunodeficiency virus protease. Antimicrob Agents Chemother 1996;40:292–7. [PubMed: 8834868]
19. Molla A, Korneyeva M, Gao Q, Vasavanonda S, Schipper PJ, Mo HM, Markowitz M, Chernyavskiy T, Niu P, Lyons N, Hsu A, Granneman GR, Ho DD, Boucher CA, Leonard JM, Norbeck DW, Kempf DJ. Ordered accumulation of mutations in HIV protease confers resistance to ritonavir. Nat Med 1996;2:760–6. [PubMed: 8673921]
20. Gong YF, Robinson BS, Rose RE, Deminie C, Spicer TP, Stock D, Colonno RJ, Lin PF. In vitro resistance profile of the human immunodeficiency virus type 1 protease inhibitor BMS-232632. Antimicrob Agents Chemother 2000;44:2319–26. [PubMed: 10952574]
21. Velazquez-Campoy A, Todd MJ, Vega S, Freire E. Catalytic efficiency and vitality of HIV-1 proteases from African viral subtypes. Proc Natl Acad Sci U S A 2001;98:6062–7. [PubMed: 11353856]
22. Ohtaka H, Schon A, Freire E. Multidrug resistance to HIV-1 protease inhibition requires cooperative coupling between distal mutations. Biochemistry 2003;42:13659–66. [PubMed: 14622012]
23. Clemente JC, Moose RE, Hemrajani R, Whitford LR, Govindasamy L, Reutzel R, McKenna R, Agbandje-McKenna M, Goodenow MM, Dunn BM. Comparing the accumulation of active- and nonactive-site mutations in the HIV-1 protease. Biochemistry 2004;43:12141–51. [PubMed: 15379553]

24. Velazquez-Campoy A, Vega S, Fleming E, Bacha U, Sayed Y, Dirr HW, Freire E. Protease inhibition in African subtypes of HIV-1. AIDS Rev 2003;5:165–71. [PubMed: 14598565]
25. Johnson VA, Brun-Vezinet F, Clotet B, Conway B, D'Aquila RT, Demeter LM, Kuritzkes DR, Pillay D, Schapiro JM, Telenti A, Richman DD. Update of the drug resistance mutations in HIV-1: 2004. Top HIV Med 2004;12:119–24. [PubMed: 15516709]
26. Muzammil S, Ross P, Freire E. A Major Role for a Set of Non-Active Site Mutations in the Development of HIV-1 Protease Drug Resistance. Biochemistry 2003;42:631–8. [PubMed: 12534275]
27. Olsen DB, Stahlhut MW, Rutkowski CA, Schock HB, vanOlden AL, Kuo LC. Non-active site changes elicit broad-based cross-resistance of the HIV- 1 protease to inhibitors. J Biol Chem 1999;274:23699–701. [PubMed: 10446127]
28. Stoll V, Qin W, Stewart KD, Jakob C, Park C, Walter K, Simmer RL, Helfrich R, Bussiere D, Kao J, Kempf D, Sham HL, Norbeck DW. X-ray crystallographic structure of ABT-378 (lopinavir) bound to HIV-1 protease. Bioorg Med Chem 2002;10:2803–6. [PubMed: 12057670]
29. Wallace AC, Laskowski RA, Thornton JM. LIGPLOT: a program to generate schematic diagrams of protein-ligand interactions. Protein Eng 1995;8:127–34. [PubMed: 7630882]
30. Schnell T, Schmidt B, Moschik G, Thein C, Paatz C, Korn K, Walter H. Distinct cross-resistance profiles of the new protease inhibitors amprenavir, lopinavir, and atazanavir in a panel of clinical samples. Aids 2003;17:1258–61. [PubMed: 12819531]
31. Colonno RJ, Thiry A, Limoli K, Parkin N. Activities of atazanavir (BMS-232632) against a large panel of human immunodeficiency virus type 1 clinical isolates resistant to one or more approved protease inhibitors. Antimicrob Agents Chemother 2003;47:1324–33. [PubMed: 12654666]
32. Colonno R, Rose R, McLaren C, Thiry A, Parkin N, Friborg J. Identification of I50L as the signature atazanavir (ATV)-resistance mutation in treatment-naive HIV-1-infected patients receiving ATV-containing regimens. J Infect Dis 2004;189:1802–10. [PubMed: 15122516]
33. Yanchunas J Jr, Langley DR, Tao L, Rose RE, Friborg J, Colonno RJ, Doyle ML. Molecular basis for increased susceptibility of isolates with atazanavir resistance-conferring substitution I50L to other protease inhibitors. Antimicrob Agents Chemother 2005;49:3825–32. [PubMed: 16127059]
34. Mahalingam B, Louis JM, Reed CC, Adomat JM, Krouse J, Wang YF, Harrison RW, Weber IT. Structural and kinetic analysis of drug resistant mutants of HIV-1 protease. Eur J Biochem 1999;263:238–45. [PubMed: 10429209]
35. Hong L, Zhang XJ, Foundling S, Hartsuck JA, Tang J. Structure of a G48H mutant of HIV-1 protease explains how glycine-48 replacements produce mutants resistant to inhibitor drugs. FEBS Lett 1997;420:11–6. [PubMed: 9450540]
36. King NM, Melnick L, Prabu-Jeyabalan M, Nalivaika EA, Yang SS, Gao Y, Nie X, Zepp C, Heefner DL, Schiffer CA. Lack of synergy for inhibitors targeting a multi-drug-resistant HIV-1 protease. Protein Sci 2002;11:418–29. [PubMed: 11790852]
37. Kempf DJ, Marsh KC, Denissen JF, McDonald E, Vasavanonda S, Flentge CA, Green BE, Fino L, Park CH, Kong XP, et al. ABT-538 is a potent inhibitor of human immunodeficiency virus protease and has high oral bioavailability in humans. Proc Natl Acad Sci U S A 1995;92:2484–8. [PubMed: 7708670]
38. Kaldor SW, Kalish VJ, Davies JF 2nd, Shetty BV, Fritz JE, Appelt K, Burgess JA, Campanale KM, Chirgadze NY, Clawson DK, Dressman BA, Hatch SD, Khalil DA, Kosa MB, Lubbehusen PP, Muesing MA, Patick AK, Reich SH, Su KS, Tatlock JH. Viracept (nelfinavir mesylate, AG1343): a potent, orally bioavailable inhibitor of HIV-1 protease. J Med Chem 1997;40:3979–85. [PubMed: 9397180]
39. Munshi S, Chen Z, Yan Y, Li Y, Olsen DB, Schock HB, Galvin BB, Dorsey B, Kuo LC. An alternate binding site for the P1-P3 group of a class of potent HIV-1 protease inhibitors as a result of concerted structural change in the 80s loop of the protease. Acta Crystallogr D Biol Crystallogr 2000;56(Pt 4): 381–8. [PubMed: 10739910]
40. Ohtaka H, Freire E. Adaptive inhibitors of the HIV-1 protease. Prog Biophys Mol Biol 2005;88:193–208. [PubMed: 15572155]
41. Ridky TW, Cameron CE, Cameron J, Leis J, Copeland T, Wlodawer A, Weber IT, Harrison RW. Human immunodeficiency virus, type 1 protease substrate specificity is limited by interactions

between substrate amino acids bound in adjacent enzyme subsites. J Biol Chem 1996;271:4709–17. [PubMed: 8617736]

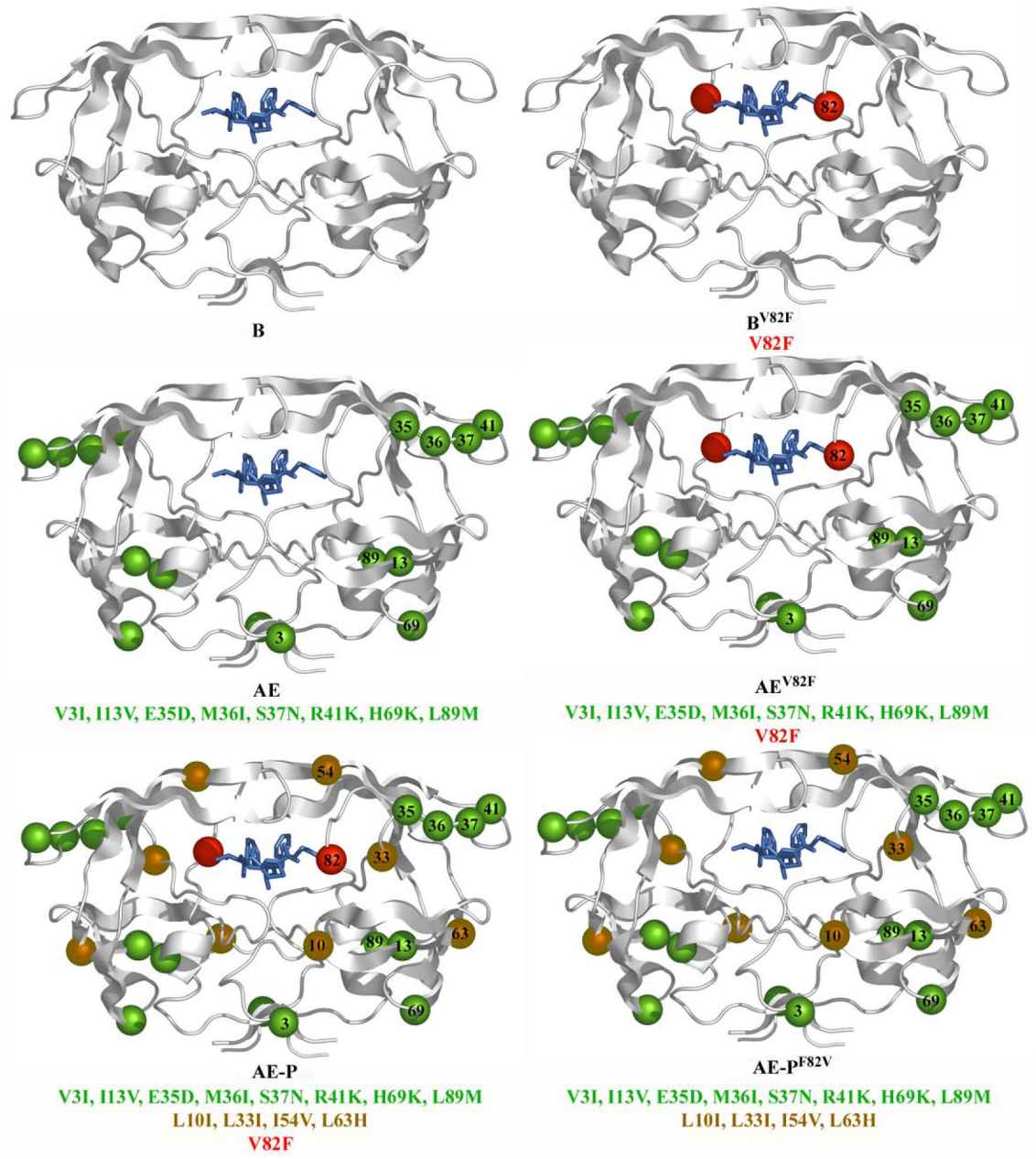

Figure 1.

Ribbon diagrams of HIV-1 proteases. Top left, pre-therapy HIV-1 subtype-B (B) protease; top right, B protease plus active site mutation V82F (B^{V82F}); middle left, pre-therapy HIV-1 CRF_01 A/E (AE) protease; middle right, AE protease plus active site mutation V82F (AE^{V82F}); bottom left, post-therapy A/E protease (AE-P); bottom right, AE-P protease with back mutation F82V ($AE\text{-}P^{F82V}$). The red sphere marks the V82F active site mutation. The green spheres mark the natural polymorphisms found in AE protease when compared to the B protease. The brown spheres mark the therapy acquired non-active site mutations in the AE-P protease.

A.

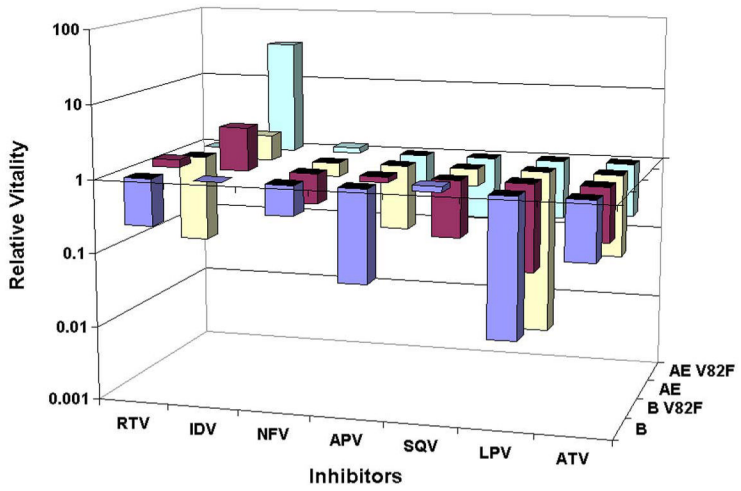

B.

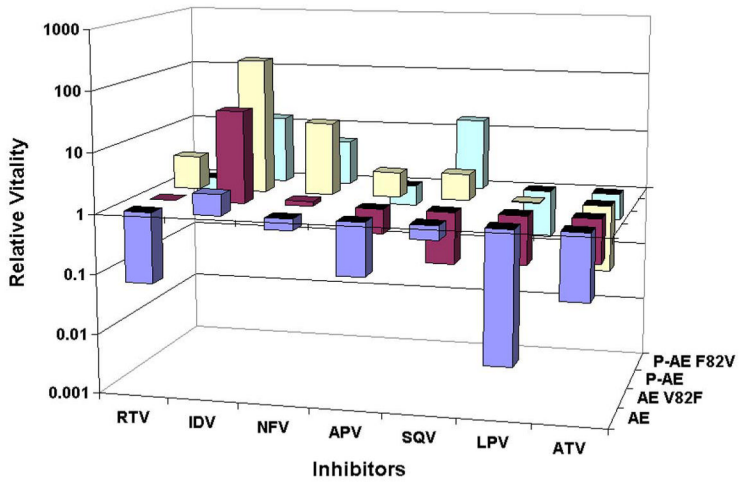

Figure 2.

Relative vitality values. (A) Relative vitality values for B, B^{V82F}, AE, and AE^{V82F} using B and K_i of IDV as reference. (B) Relative vitality values for AE, AE^{V82F}, AE-P, and AE-P^{F82V} using AE and K_i of IDV as reference.

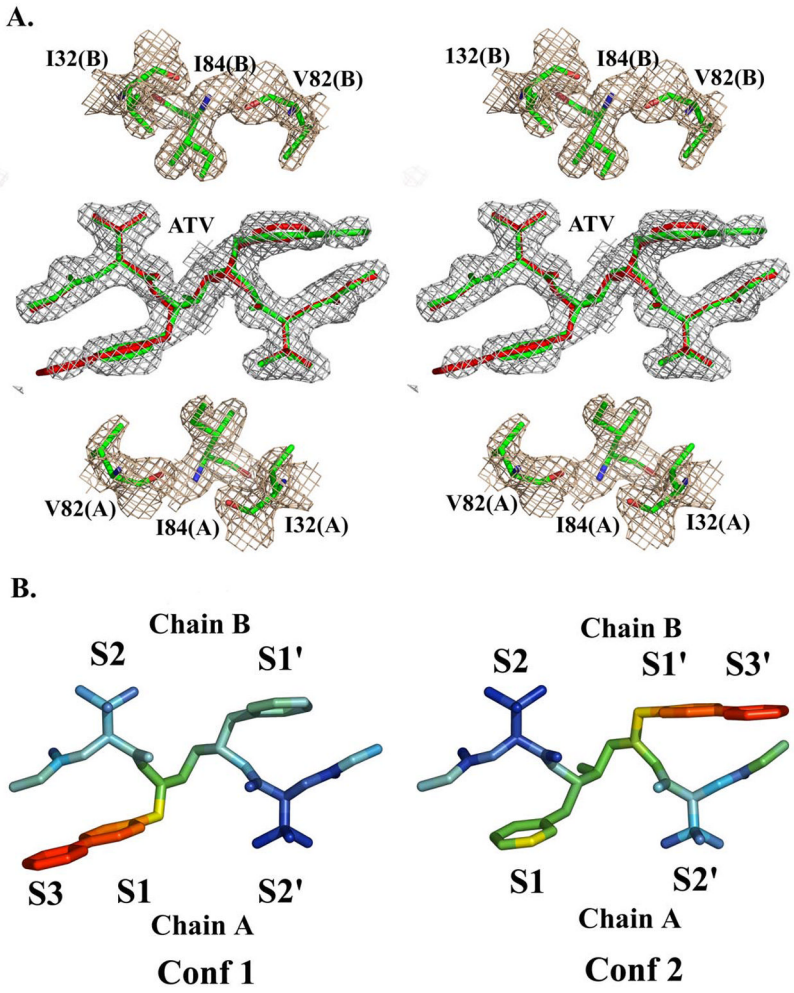

Figure 3.

(A) Stereo view of ATV in the active site. Conformation-1 (Conf1) (red) and Conformation-2 (Conf2) (green) are shown as sticks. Residues Val32(A), Val82(A), and Ile84(A) in chain A, and Val32(B), Val82(B), and Ile84(B) in chain B are shown as green sticks. 2FoFc electron density is drawn as a beige mesh at 1σ level. (B) Stick drawing of ATV Conf1 and 2 colored by B-values with red highest and blue lowest.

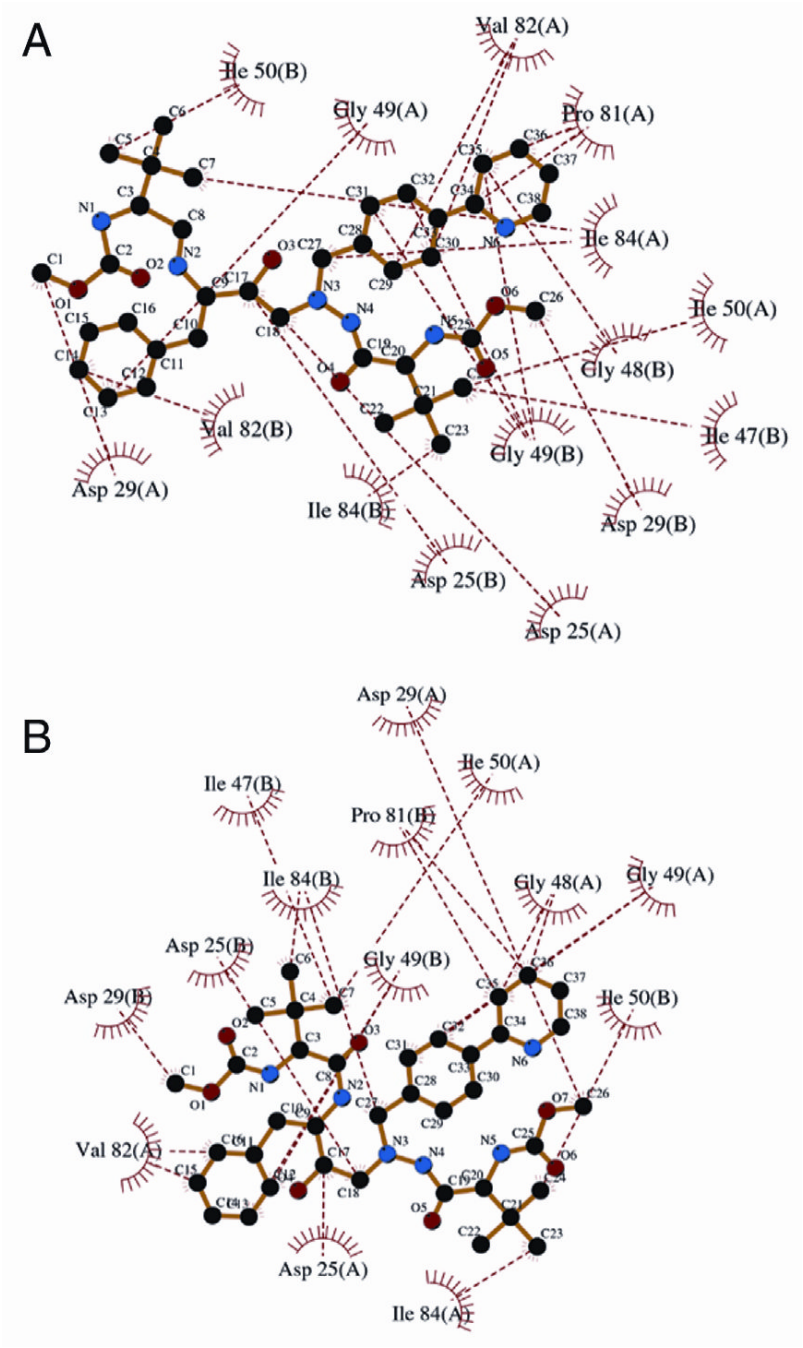

Figure 4.

Ligplot two dimensional representation of hydrophobic interactions of ATV with active site residues for ATV in (panel A) Conf1 and (panel B) Conf2. Hydrophobic interactions with residues in the first monomer [e.g., Gly 49(A)] and the second monomer [e.g., Ile 50(B)] are shown as red dashed lines.

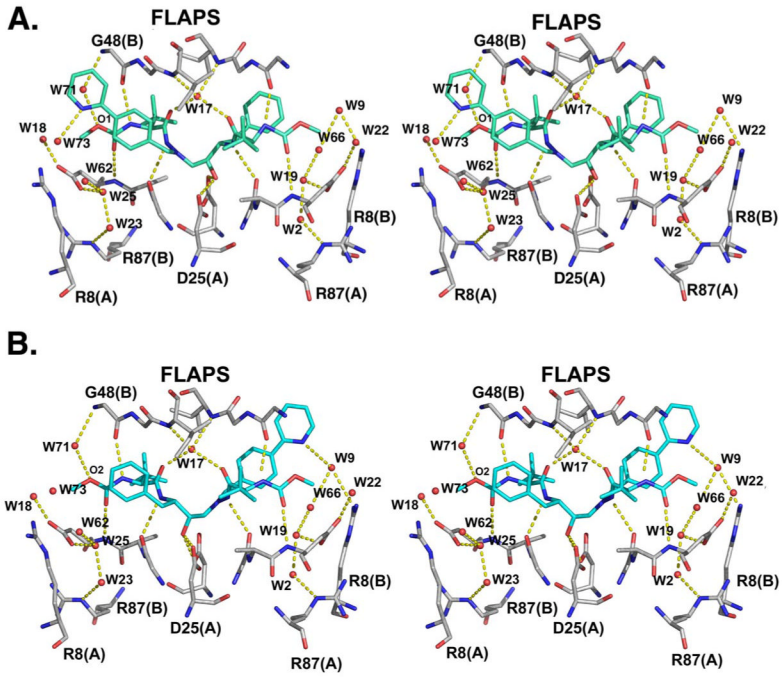

Figure 5.

Stereo view of hydrogen bonding interactions of ATV for (A) Conf1 (green) and (B) Conf2 (aqua). Flap and active site residues are drawn as CPK sticks. Key residues described in the text are labeled. Hydrogen bonds are shown as yellow dashes. Water molecules are drawn as red spheres.

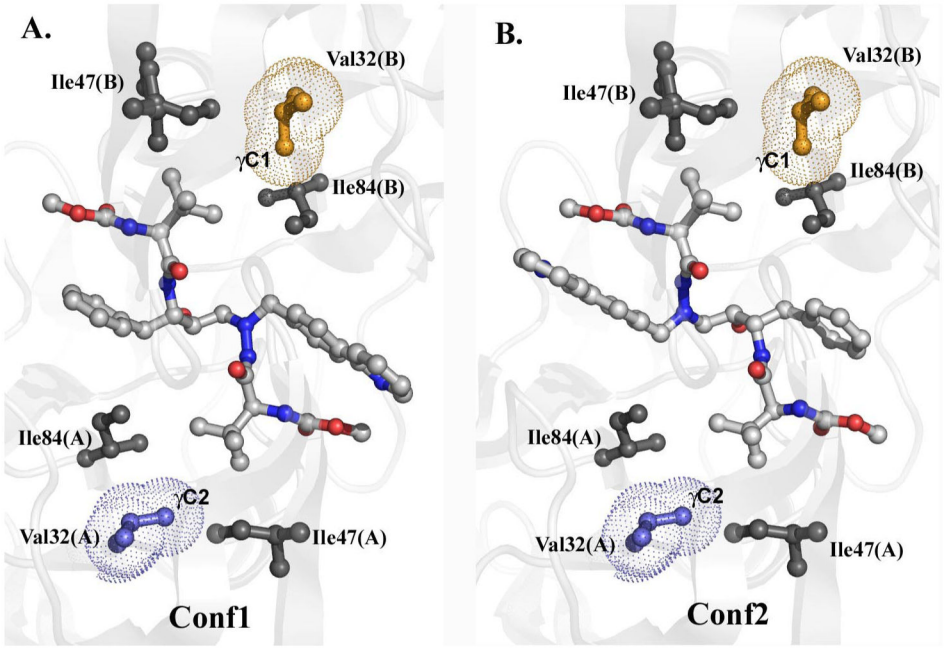

Figure 6.
Interactions of residues Val32, Ile47, and Ile84 in inhibitor Conf1 (panel A) and Conf2 (panel B). In both panels, residues Ile84 and Ile47 (gray), Ile32(A) (blue), Val32(B) (orange), and inhibitor are modeled as ball and sticks.

Table 1

Michaelis-Menten Constants

Variants*	K_m (μM)	k_{cat} (sec^{-1})	k_{cat}/K_m ($\mu M^{-1}sec^{-1}$)
(S1) K-A-R-V-L * nF-E-A-nL-G			
B	18 ± 2	20 ± 1	1.2 ± 0.2
B^{V82F}	18 ± 2	7.3 ± 0.8	0.40 ± 0.05
AE	15 ± 2	8.2 ± 0.5	0.54 ± 0.07
AE^{V82F}	62 ± 8	11 ± 1	0.17 ± 0.02
AE-P	29 ± 3	11 ± 1	0.38 ± 0.04
$AE\text{-}P^{F82V}$	20 ± 3	8.9 ± 0.7	0.44 ± 0.07
(S2) K-A-R-V-nL * nF-E-A-nL-G			
B	10 ± 1	9.0 ± 0.6	0.9 ± 0.1
B^{V82F}	29 ± 5	9 ± 1	0.31 ± 0.05
AE	15 ± 3	16 ± 1	1.1 ± 0.2
AE^{V82F}	32 ± 3	6.7 ± 0.6	0.21 ± 0.02
AE-P	31 ± 3	10 ± 1	0.32 ± 0.03
$AE\text{-}P^{F82V}$	67 ± 7	16 ± 1	0.24 ± 0.03
(S3) K-A-R-V-F * nF-E-A-nL-G			
B	6.2 ± 0.6	9.0 ± 0.3	1.5 ± 0.1
B^{V82F}	17 ± 2	6.4 ± 0.7	0.38 ± 0.04
AE	9 ± 1	15 ± 1	1.7 ± 0.2
AE^{V82F}	41 ± 3	14 ± 1	0.33 ± 0.02
AE-P	12 ± 2	13 ± 1	1.0 ± 0.2
$AE\text{-}P^{F82V}$	20 ± 3	11 ± 1	0.5 ± 0.1

*B, pre-therapy HIV-1 subtype-B protease; B^{V82F}, B protease plus active site mutation V82F; AE, pre-therapy HIV-1 CRF_01 A/E protease; AE^{V82F}, AE protease plus active site mutation V82F; AE-P, post-therapy HIV-1 CRF_01 A/E protease; $AE\text{-}P^{F82V}$, AE-P protease with back mutation F82V.

Table 2

Ki values (nM)

Variants	RTV	IDV	NFV	APV	SQV	LPV	ATV
B	0.7 ± 0.1	3.1 ± 0.1	1.2 ± 0.2	0.17 ± 0.01	1.3 ± 0.3	0.05 ± 0.02	0.48 ± 0.06
B^{V82F}	4 ± 1 (6)	12 ± 1 (4)	1.2 ± 0.3 (1)	2.6 ± 0.4 (15)	0.52 ± 0.13 (−3)	0.2 ± 0.05 (5)	0.56 ± 0.03 (1)
AE	0.2 ± 0.1 (−4)	6.9 ± 0.3 (2)	2 ± 0.3 (2)	0.4 ± 0.1 (2)	1.8 ± 0.3 (0)	0.019 ± 0.004 (−2)	0.24 ± 0.07 (−2)
AE^{V82F}	3.1 ± 0.6 (4)	108 ± 12 (35)	3.7 ± 0.5 (3)	1.2 ± 0.2 (7)	0.43 ± 0.07 (−3)	0.48 ± 0.1 (12)	0.57 ± 0.19 (1)
AE-P	32 ± 3 (46)	1616 ± 119 (521)	146 ± 12 (122)	23 ± 3 (135)	24 ± 3 (18)	9 ± 1 (180)	0.7± 0.2 (1)
$AE\text{-}P^{F82V}$	1.2 ± 0.4 (2)	42 ± 6 (14)	17 ± 3 (14)	1.4 ± 0.4 (8)	48 ± 8 (38)	0.5 ± 0.1 (10)	1.1± 0.3 (2)

The +/− fold change in Ki from B are shown in parenthesis

RTV=ritonavir, IDV=indinavir, NFV=nelfinavir, APV=amprenavir, SQV=saquinavir, LPV=lopinavir, AZV=atazanavir

Table 3

X-ray data collection and refinement statistics

wavelength (Å)	1.1
resolution range (Å)	20-2.0
space group	$P6_1$
unit-cell parameters *a*, *c* (Å)	62.4, 82.6
number of reflections	49,001
number of unique reflections	12,351
overall completeness (%)	99.8 (100)
average I/σ	8.1
[1] R_{sym} (%)	8.4 (47.2)
Refinement Statistics	
[2] R_{work} (%)	22.7 (29.6)
[3] R_{free} (%)	23.8 (30.2)
rmsd bond length (Å)	0.02
rmsd bond angle (Å)	2.3
Average B factor (Å^2)	
Wilson Plot	35.3
Protein main/side chains	29.0/32.7
inhibitor atoms	28.3
water molecules	37.1
Ramachandran plot quality	
most favored (%)	94.9
additionally allowed (%)	5.1
generously allowed (%)	0
disallowed (%)	0

[1] $R_{sym} = \Sigma_i hkl|I(hkl) - I_i(hkl)|i,hkl/I_i(hkl)*100$. Where $I_i(hkl)$ is the ith observation of the intensity of a reflection with indices h,k,l and <I(hkl)> is the average intensity of all symmetry equivalent measurements of that reflections.

[2] $R_{work} = \Sigma_i(hkl)Fobs(h)| |Fcalc(h)/(hkl)|Fobs(h)|*100$. Where Fobs(h) and Fcalc(h) are the observed and calculated structure factor amplitudes respectively.

[3] $R_{free} = \Sigma_i(hkl)TFobs| |Fcalc/(hkl)T|Fobs|*100$. Rfree is calculated using 5% of data excluded during refinement process. Statistics for the highest resolution shell are given in parenthesis.